

Journal of Biomedical Optics

SPIEDigitalLibrary.org/jbo

Photo-sensitive hydrogels for three-dimensional laser microfabrication in the presence of whole organisms

Jan Torgersen
Aleksandr Ovsianikov
Vladimir Mironov
Niklas Pucher
Xiaohua Qin
Zhiquan Li
Klaus Cicha
Thomas Machacek
Robert Liska
Verena Jantsch
Jürgen Stampfl

Photo-sensitive hydrogels for three-dimensional laser microfabrication in the presence of whole organisms

Jan Torgersen,^a Aleksandr Ovsianikov,^a Vladimir Mironov,^a Niklas Pucher,^b Xiaohua Qin,^b Zhiquan Li,^b Klaus Cicha,^a Thomas Machacek,^c Robert Liska,^b Verena Jantsch,^c and Jürgen Stampfl^a

^aVienna University of Technology, Institute of Materials Science and Engineering, Favoritenstrasse 9-11, 1040 Vienna, Austria

^bVienna University of Technology, Institute for Applied Synthetic Chemistry, Getreidemarkt 9, 1060 Vienna, Austria

^cUniversity of Vienna, Department of Chromosome Biology, Max F. Perutz Laboratories, Dr. Bohr-Gasse 1, 1030 Vienna, Austria

Abstract. Hydrogels are polymeric materials with water contents similar to that of soft tissues. Due to their biomimetic properties, they have been extensively used in various biomedical applications including cell encapsulation for tissue engineering. The utilization of photopolymers provides a possibility for the temporal and spatial controlling of hydrogel cross-links. We produced three-dimensional (3-D) hydrogel scaffolds by means of the two-photon polymerization (2PP) technique. Using a highly efficient water-soluble initiator, photopolymers with up to 80 wt.% water were processed with high precision and reproducibility at a writing speed of 10 mm/s. The biocompatibility of the applied materials was verified using *Caenorhabditis elegans* as living test organisms. Furthermore, these living organisms were successfully embedded within a $200 \times 200 \times 35 \mu\text{m}^3$ hydrogel scaffold. As most biologic tissues exhibit a window of transparency at the wavelength of the applied femtosecond laser, it is suggested that 2PP is promising for an in situ approach. Our results demonstrate the feasibility of and potential for bio-fabricating 3-D tissue constructs in the micrometre-range via near-infrared lasers in direct contact with a living organism. © 2012 Society of Photo-Optical Instrumentation Engineers (SPIE). [DOI: 10.1117/1.JBO.17.10.105008]

Keywords: bio-fabrication; hydrogel; photoinitiator; photopolymers; two-photon polymerization.

Paper 12115 received Feb. 17, 2012; revised manuscript received Jul. 31, 2012; accepted for publication Sep. 7, 2012; published online Oct. 15, 2012.

1 Introduction

The classic approach for the realization of bioartificial tissues suitable for clinical implantation is based on cell seeding onto a three-dimensional (3-D) porous supporting structure. These constructs, so-called scaffolds, consist of natural or synthetic biodegradable biomaterials.¹⁻³ Scaffolds define the configuration and the overall 3-D shape of the tissue substitute, provide appropriate support for cell proliferation, determine desirable material properties of tissue constructs, can deliver biologic signalling molecules, and facilitate the directed differentiation of seeded cells.⁴

Additive manufacturing techniques (AMT) have found increasing interest to serve as methods for 3-D scaffold fabrication. The constructs can be produced reproducibly and in accordance to a computer-aided design (CAD) model.^{5,6} The cells can be introduced by two different ways into the scaffold: (a) seeding of cells onto the surface after the fabrication; or (b) incorporation of cells into the fabrication process.^{7,8}

Tissue isolation and seeding processes, required for an introduction of cells on the constructs after the fabrication, can lead to a loss of many important aspects of cell-cell interactions.⁹ Furthermore it is difficult to obtain uniform cell seeding, as most of the cells seed in the periphery. In contrast, the incorporation into the material during the fabrication process allows higher cell densities and better control over the distribution.⁷ However, it requires materials that support the viability of cells. Hydrogels, stable cross-linked hydrophilic polymeric

networks, are similar to body tissue¹⁰ and serve as suitable matrices for cell encapsulation and culture.¹¹

So far, AMT such as fused deposition modelling and selective laser sintering have been used to fabricate 3-D scaffolds.^{12,13} However, these techniques do not allow the incorporation of cells due to intrinsic technological limitations (high temperature).⁵ In contrast, photopolymerization can be done in the presence of cells. In this context, stereolithography was used to fabricate 3-D constructs from cell-containing formulations with water content.^{14,15} However, common AMT alone cannot meet the requirements of mimicking the complexity of natural cell environment¹⁶: they are inherently two-dimensional (2-D) and require manual layer-by-layer processing to prepare 3-D scaffolds,¹⁷ the resolution is limited to a few tens of micrometres.^{18,19} In addition, photopolymerization based methods use UV light, which might induce DNA damage in living cells.²⁰

In contrast, 3-D two-photon polymerization (2PP) of scaffolds²¹⁻²⁴ offers:

- (1) True 3-D structuring without the necessity of layer-by-layer manufacturing.²⁵ As polymerization does not occur on the surface of the polymerizable formulation, all shortcomings related to the formation of the working surface can be discarded, such as resolution limiting surface tensions,²⁶ the need of supporting material,²⁷ and oxygen inhibition.²⁸ Furthermore, 2PP is capable of embedding objects.²⁹

Address all correspondence to: Jürgen Stampfl, Vienna University of Technology, Institute of Materials Science and Engineering, Favoritenstrasse 9-11, 1040 Vienna, Austria. Fax: +43 (0)15880130895; E-mail: jstampfl@pop.tuwien.ac.at

- (2) Scalable spatial resolution via appropriate focusing optics and laser irradiation parameters. Structures with feature sizes ranging from 65 nm³⁰ to hundreds of micrometres may be produced.³¹ Using 2PP it is possible to reproducibly replicate structures at scales suitable for a host of tissue engineering applications (0.1 to 10 μm to control the microenvironment of individual cells, 10 to 400 μm to control the structure of clustered cells and >400 μm to control the interactions between multiple cell clusters).⁹
- (3) Processing with light emitted in the near infrared (NIR) spectral range. Nonlinear absorption provides the effect of short wavelength excitation inside the focal point,^{32,33} the specimen is only exposed to light of moderate average power. Absorption sufficiently high to produce two-photon excitation occurs in the immediate vicinity of the focal point of a light beam of appropriate energy only.³³ This effect avoids photoactivation of the initiator outside the focal volume rendering the processed materials transparent for the NIR beam.³³ Femtosecond laser irradiation at 800 nm can be used in the presence of cells without a negative impact.^{34,35}

The successful 2PP microfabrication of cytocompatible hydrogel scaffolds was recently reported.^{21,36} These structures can be developed in aqueous media and subsequently seeded with cells. However, the incorporation of cells into the fabrication process requires higher water contents⁷ and hence a water-soluble 2PP photoinitiator. Irgacure 2959 commonly used for cell encapsulation in hydrogels is only suitable for 2PP at 515 nm.²¹

However, the opacity of living tissues in the visible wavelength range limits the *in vivo* use of photoresponsive hydrogels.¹⁰ NIR lasers have the potential to overcome this restriction, because most cells and tissues are transparent for NIR.³² Recently reported, NIR light has been transmitted deeply into biological tissues without causing damage, permitting the accumulation of nanogels at laser-irradiated sites in mice.³⁷ At 800 nm wavelength, commercially available, water-soluble xanthene sensitizers were used to initiate 2PP.³⁸ In a recent work, 3-D matrices could be cross-linked from cytoplasmic proteins in a live cell (starfish oocyte).³⁹ These findings show that 2PP 3-D microfabrication works in a biological environment. Xanthene dyes like Rose Bengal, however, have small two-photon absorption (2PA) cross-sections of 10 Göppert-Meyer (GM) at 800 nm.⁴⁰ High laser intensities and long exposure times are required. A high performing, water-soluble 2PP initiator, similar to Irgacure 2959 but suitable for 800 nm wavelength, would facilitate an effective, high precision and fast microfabrication in a biologic surrounding.

Here we introduce a water-soluble, 2PA initiator (WSPI). The initiator and its derivatives were described for the use in two-photon microscopy.⁴¹ In this paper, it was synthesised and slightly adapted for the use with 2PP. The reported high 2PA cross-section of 120 GM at 800 nm favors high initiating efficiency.⁴¹

For any successful *in vivo* application, however, biocompatibility on cellular, tissue and organism level is essential*. Testing is mostly done using cultured cells, but this requires an

expensive infrastructure. In addition, stress responses in cells are often not visible via direct microscopic observation and cell viability cannot be easily defined in terms of a single physiological or morphological parameter.⁴² Before investing in cell laboratories, employ biologists and adapt machines to fit biological conditions, therefore, material and chemistry labs have to predetermine the biocompatibility of their materials and methods. Because of their easy maintenance, multi-cellular organisms are becoming popular as prescreening models. Bioelectrosprayed multicellular zebrafish embryos, for example, have recently served as efficient biosensors for investigating the biocompatibility of electrospaying.⁴³

Caenorhabditis elegans (*C. elegans*) can serve as inexpensive and ethically acceptable high-throughput and real-time biosensor for animal organisms in predicting acute lethality in mammals.⁴⁴ Several publications focus on the effects of chemicals on wild-type nematode survival (LC₅₀), development and mutagenicity.⁴⁵⁻⁴⁷ As *C. elegans* uses chemosensation to find food, avoid noxious conditions, develop appropriately and mate, it has to sense chemicals that penetrate the cuticle, exposing its sensory cilia to the environment.⁴⁷ We consider the choice of *C. elegans* as a model organism appropriate to provide the practical basis for a proof of concept for applying 2PP in a biological surrounding.

In what follows, we will evaluate the behavior of hydrogel structures fabricated with 2PP in formulations with high water content. We will discuss the impact on the structures' dimensions deriving from the amount of water in the formulation and the applied laser power for the structuring at a given fabrication speed. We will investigate the impact of laser power and structuring speed for fabricating CAD scaffolds in formulations with different 50% and 80% water contents, respectively, showing the 3-D capabilities of the presented approach. We continue with LC₅₀ assays demonstrating the biocompatibility of the presented formulations and we will briefly review the advantages of using NIR light for biofabrication. Finally, we will show 3-D biofabrication in the presence of living organisms.

2 Materials and Methods

2.1 Two-Photon Polymerization

The 2PP setup is shown in Fig. 1. A 100-fs pulsed, 810 nm laser beam of a Ti:sapphire laser (high Q laser) with a repetition rate of 73 MHz and 400 mW power output passed through an acousto-optic modulator leaving the first order of diffraction for the structuring. A $\lambda/2$ waveplate in combination with a

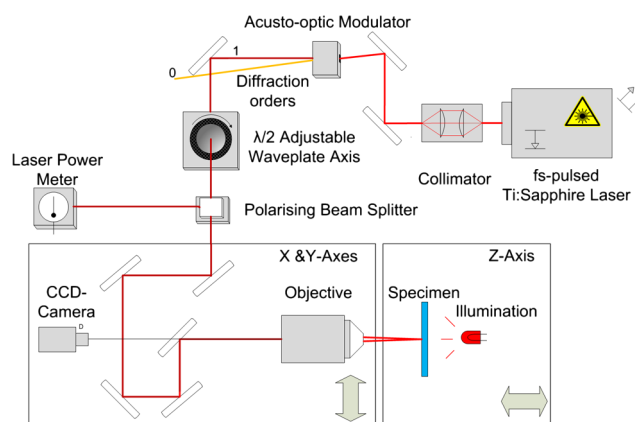


Fig. 1 Scheme of the 2PP setup used for the experiments in this work.

*We will further refer to the biocompatibility as "the quality of not having toxic or injurious effects on biological systems."⁵⁷

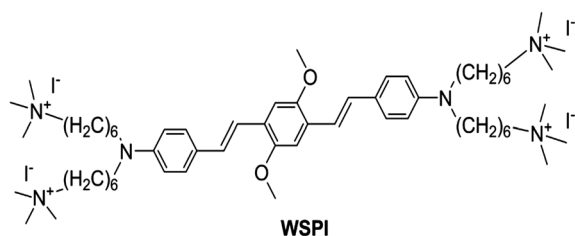


Fig. 2 The molecular structure of WSPI: high 2PA and good water solubility.

polarising beam-splitter adjusted the intensity. Two high precision air bearing axes (Aerotech) moved the beam focusing microscope objective in the X and Y -dimension. A $20\times$ microscope objective (NA 0.4; Zeiss LD Plan-Neofluar) focused the beam into the formulation. The formulation container was mounted on the Z -Axis (Aerotech). For the online process observation, a camera viewed along the laser beam and got focused on the polymerization spot through the same objective. The axes were mounted on a hard stone frame designed to damp vibrations.

2.2 Two-Photon Active, Water-Soluble Initiator WSPI and Monomers

The water-soluble two-photon active molecule, 1,4-bis(4-(N,N-bis(6-(N,N,N-trimethylammonium)hexyl)amino)-styryl)-2,5-dimethoxybenzene tetraiodide (WSPI, Fig. 2), used for 2PP hydrogel applications was synthesised according to a protocol published previously.⁴¹ The 4,4'-dialkylamino bis(styryl)benzene core was prepared by Horner-Wadsworth-Emmons (HWE) reaction of appropriate HWE phosphonate and aldehyde. The water-soluble functional moiety was introduced in the final synthesis step via quarternization reaction using trimethylamine.

The 4,4'-dialkylamino bis(styryl)benzene core with large 2PA cross-section of 120 GM was reported previously.^{41,48} The additional quaternary ammonium cations enable good solubility in water. The charged end groups bonded to the aniline functionality via long aliphatic chains do not appear to interact with the electronic structure of the two-photon active chromophore, and thus do not affect its photobehavior.

It has to be mentioned that the analogue of WSPI 4,4'-dialkylamino bis(styryl)benzene has also been employed as a potent two-photon active initiator for 2PP through bimolecular electron transfer process from photoexcited chromophores to acrylate monomers.⁴⁸ As a monomer we used poly(ethylene glycol) diacrylate (PEGda) with a molecular mass of 700 Da (Sigma-Aldrich 45008). Four formulations with varying PEGda concentrations were prepared (50, 40, 30, and 20 wt.%). For 2PP structuring, 2 wt.% of WSPI was added to each formulation.

2.3 Fabrication of 3-D Structures by Means of 2PP

Prior to 3-D structuring, likely deviations were predetermined structuring CAD rods shown in Fig. 3(a) at different laser doses in formulations with different water contents (50%, 60%, 70%, and 80%, respectively). This was done at 10 mm/s of writing speed and laser powers ranging from 140 mW to 260 mW at an increment of 20 mW.

To investigate the photosensitivity and the 3-D capabilities of the presented formulations, we determined appropriate structuring windows fabricating scaffolds according to Fig. 3(b). Twenty-one 3-D CAD scaffolds [Fig. 3(b)] were structured at different laser energy doses in two formulations containing the lowest (50%) and the highest (80%) water contents of the presented formulations, respectively. This could be done altering the laser power (60 to 300 mW by steps of 40 mW) and the fabrication speed (1 \times to \times 10 mm/s by steps of 3 mm/s).

2.4 Sample Development and Analysis of 2PP Structures

After fabrication, the structures were rinsed with M9 buffer to get rid of monomer residues. The structures swell in water, after 24 h in M9 they reach equilibrium absorption. The rod structures were observed via laser scanning microscopy (LSM) using a $50\times$ NA 0.8 objective (488-nm laser, Zeiss LSM 700). The dimension of a polymer line was calculated using the fluorescence distribution over the distance of the scanned plane. The width was considered as the distance from the first point with fluorescence intensity above 10% of the maximum to the point where intensity fell below 10% of the maximum. Optical measurements were done for validation (see Appendix).

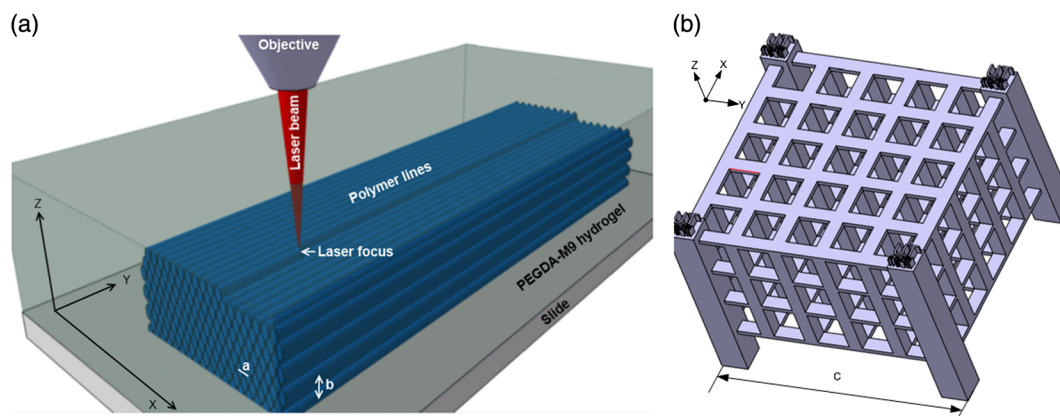


Fig. 3 Schematic drawing of 2PP fabrication; (a) the CAD file of the rods ($15 \times 140 \times 21 \times \mu\text{m}^3$ X/Y/Z) was sliced into layers at a distance of $3.5 \mu\text{m}$ (labeled b) to each other. One layer's area was made out of 19 polymeric lines at equal spaces of $0.8 \mu\text{m}$ (labeled a) to each other; (b) CAD of scaffold $280 \times 280 \times 225 \times \mu\text{m}^3$ (line distance $0.3 \mu\text{m}$, layer distance $3 \mu\text{m}$).

Due to their height, the 3-D scaffolds could not be investigated using the 50× NA 0.8 objective of the LSM (limited working distance). A 20× NA 0.5 objective was used (488-nm laser, Zeiss LSM 700). The scaffolds were optically assessed following previous protocols.^{49,50}

2.5 Preparation of a Synchronized *C. elegans* Population

C. elegans was cultured using standard techniques.⁵¹ The N2 Bristol *C. elegans* strain was synchronized via hypochlorite digestion of worms, with only eggs surviving. Unstaged *C. elegans* cultures with adults were incubated for 5 min in bleaching solution (10% 5 M NaOH, 20% chlorine bleach) until adult worm corpses were completely dissolved. Eggs were collected by centrifugation (3400 g, 2 min, 20°C, Hermle Z383K), washed with M9 buffer and seeded onto fresh plates. After letting worms hatch and grow to adulthood, worms were washed off the plates with M9 buffer.

2.6 Lethal Concentration Assay

Five-hundred microliter of a synchronized population (see Sec. 2.5) of adult N2 wild-type *C. elegans* in M9 buffer (15 worms/ μL) were pipetted into a centrifuge tube containing 500 μL of double-concentrated formulation (without initiator). The reference tube contained 500 μL worm suspension and 500 μL M9 buffer. After 15 min of exposure, the emulsion was centrifuged (3400 g, 2 min, 20°C, Hermle Z383K). The pellet was washed with 4 mL M9 buffer and centrifuged. 20 μL of cleaned worm pellet (300 to 400 worms) were pipetted onto three 35-mm agar Petri-dishes each.

The biocompatibility of the initiator was investigated separately. Four wt.% of WSPI (double the amount used for structuring) was dissolved in M9 buffer, mixed with the worm emulsion and treated equally.

Two high-resolution photographs were taken every 3 min from each dish for 18 min. The agar lawn of the petri dish absorbed the liquid leaving the worms on the lawn. Viability was determined measuring the worms' mobility and impetus to move.⁵² Comparing photographs taken at different times, visibly moving worms were considered alive.

2.7 Embedding *C. elegans* in a 3-D Woodpile Structure

A 15-mg droplet of aqueous M9 buffer containing *C. elegans* was mixed with double-concentrated hydrogel (100% PEGda, 4 wt.% WSPI) at a ratio of 1:1 rendering a formulation with 50% water content containing *C. elegans*. A woodpile structure ($200 \times 200 \times 35 \mu\text{m}^3$ X/Y/Z, 10 layers at a distance of 3.5 μm , 50 polymer lines per layer) was fabricated around a living nematode at 10 mm/s. The focal point was traced through the animal's body attaching the polymer lines to the cuticle. The specimen was developed and analyzed according to Sec. 2.4.

3 Results

3.1 2PP Microfabrication

Structuring parameters and behavior of PEGda formulations are presented. The formulations were photopolymerized using the water soluble, two-photon initiator WSPI. In preliminary tests (data not shown), no significant difference was found structuring monomers dissolved in water compared with monomers dissolved in M9 buffer, a standard media for maintaining *C. elegans*.⁵⁰

LSM images [Fig. 4(a)] show rods fabricated in hydrogel formulations (parameters described in Sec. 2.3). The water content was 50% up to 80% and 2 wt.% of WSPI was added and the writing speed was 10 mm/s. No stable structures could be obtained in formulations with 90% water content. Average laser powers ranged from 160 to 260 mW (measured before the objective). The initiator content and the LSM measuring parameters were kept constant in the experiments. The fluorescence of structures with varying monomer contents and laser powers was analyzed. Different levels of fluorescence thus can be attributed to a difference in the density of the polymer network resulting from the monomer contents and the laser powers applied during structuring.

The structures' width deviations are plotted against the average laser power applied [Fig. 4(b)]. As expected, an increase in width can be observed with an increase of the intensity applied. This is in good agreement with previous work²⁵ and can be explained with the increase of the 2PA affected zone of the focal point (volumetric pixel) with increasing laser intensity. The larger the volumetric pixel, the thicker the polymer lines and the larger the dimensions of the fabricated 3-D construct.

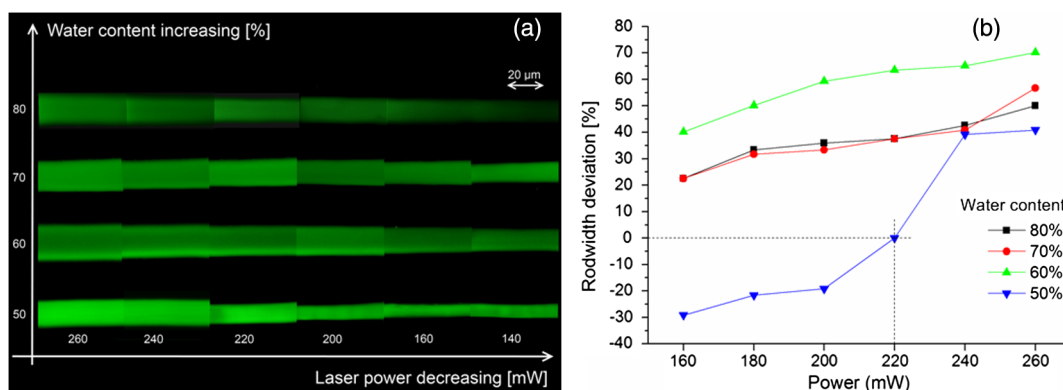


Fig. 4 (a) Rods structured using different water contents and average laser powers (LSM images, 50×); 6 objects were fabricated with power set between 260 mW and 160 mW by steps of 20 mW; and (b) width swelling ratios at different water contents and fabrication powers (LSM measurements); the CAD design width was 15 μm .

Comparing four formulations with different water contents, the largest width deviation compared to the CAD model can be seen in formulations with 60% water content (+70% width increase at 260 mW). Rods fabricated in formulation with 70% and 80% water content show a minor dimension deviation. Formulations with 50% water content; however, facilitate the fabrication of parts with the best agreement to the CAD model (best fit at 220 mW).

The different dimensions obtained in formulations with different water contents can be explained with the polymeric cross-linking density of the fabricated parts. A high monomer content of 50% renders a stiff network which absorbs little water. The auto-fluorescence of the observed parts is higher in the LSM. Defined structures with single polymer lines are visible. At 60% water content, the polymer's cross-linking density is still high but the network is more permeable increasing the water absorption. At even higher water contents (70% and 80%); the cross-linking density gets lower rendering the construct's outer contour polymer lines oligomerized. The oligomerized monomers can diffuse in the surrounding making the polymer lines thinner. The effects of monomer concentration and laser power are complex and thus cannot be said to be fully inverted.

3.2 3-D Structuring

To investigate the differences in the photoreactivity and in the 3-D capabilities of two formulations with 50% and 80% water contents, respectively, CAD scaffolds were fabricated at different parameters according to Sec. 2.3. A lower threshold where polymerization can be primarily observed at a given fabrication speed,⁵³ as well as an appropriate structuring window⁵⁰ could be found.

Figure 5 illustrated that stable structures are obtained at 60 mW at 1 mm/s, 100 mW at 4 mm/s, 140 mW at 7 mm/s, and 220 mW at 10 mm/s, respectively. Below these thresholds, polymerization is still possible, though the polymeric network is not stiff enough to keep the fabricated part in the preformed

shape. At 60 mW and fabrication speed above 7 mm/s, no polymerization is obtained. Above 260 mW and at 1 mm/s, the energy dose is too high resulting in damage to the structure and its loss of adhesion to the glass slide. Similarly, the energy dose is too high at 300 mW and 4 mm/s.

At low energy doses, the pillows attached to the glass still remain (e.g., at 100 mW, 10 mm/s). The fabricated logos with details in the μm region on the pillows (see details in Fig. 5), are pronounced in nearly all scaffolds. Yet the freely suspended parts of the structure are not stable enough and therefore deform and lose their adhesion to the pillows under their own weight.

Some of the connectors appear wavy and thin most distant from the pillows. As every layer of a structure is created line-by-line, the connector is growing in thickness during the fabrication process. Commencing the fabrication, it consists of one single line and 50 lines in the end (connector thickness $15 \mu\text{m}$ divided by line distance $0.3 \mu\text{m}$). Thus, the connector is weak at the beginning getting its full strength in the end. This can result in a deformation of single lines during the fabrication process. At higher energy doses, however, the deviation is less.

3.3 80% Water Content

Figure 6 illustrates the fabrication of scaffolds in formulations containing 80% water. The process window is shifted. Stable structures are obtained above 180 mW at 1 mm/s, 220 mW at 4 mm/s, and 300 mW at 7 mm/s, respectively. At 10 mm/s, polymerization is still possible. However, the freely suspended parts are not stiff enough and deform similar to processing formulations with higher monomer content at low energy doses. Here, the deformation of the connectors is more obvious. As previously described, the connectors grow during the fabrication process. Processing formulation with higher water content, the single polymer lines are weaker and thus the deformation is larger. The longer the fabrication process, the more time for the deformation. At higher speed and higher power, the structures would thus more fit to the CAD. The structure fabricated at 1 mm/s and 300 mW is stable (see 3-D stacked LSM image

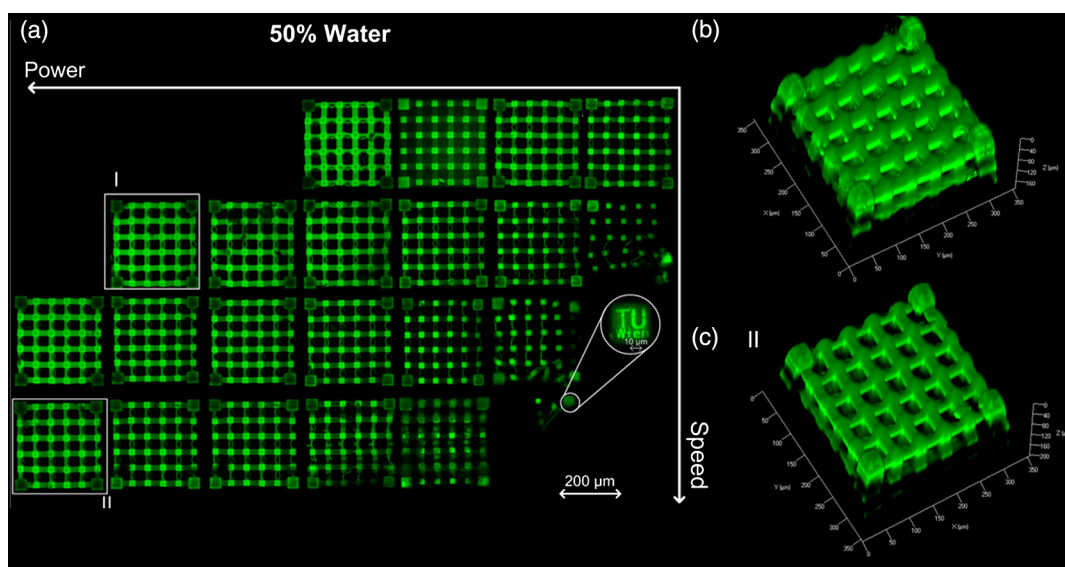


Fig. 5 (a) Speed power array of fabricated scaffolds according to 2.3; formulation containing 50% water; horizontal left to right: 300 to 60 mW by steps of 40 mW, vertical top down: 1 \times to 10 mm/s by steps of 3 mm/s, LSM images 20 \times ; and (b) stacked 3-D LSM image of white marked scaffold in (a).

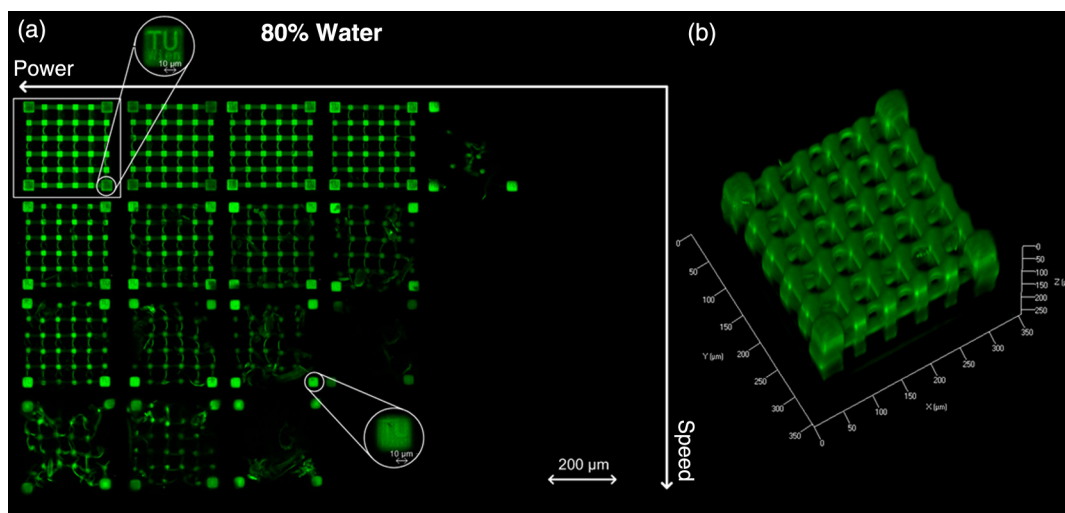


Fig. 6 (a) Speed power array of fabricated scaffolds according to 2.3; formulation containing 80% water; horizontal left to right: 300 to 100 mW by steps of 40 mW, vertical top down: 1–10 mm/s by steps of 3 mm/s, LSM images 20 \times ; and (b) stacked 3-D LSM image of white marked scaffold in (a).

in Fig. 6). No damage resulting from the laser power is recognizable. Thus, the fabrication of scaffolds at higher writing speed is probably possible at higher laser power than the current 300 mW limitation of the setup.

3.4 Biocompatibility (LC) Assay

We determined the biocompatibility of the used compounds with decreasing monomer concentrations. As previously reported,⁵² we employed a movement assay for adverse effects on exposed animals. We define an animal as dead when it completely lacked motion after a recovery phase of 20 min. The duration of this phase has been shown to be sufficient to exclude the possibility of nonmoving but living animals regaining their mobility. A 1:1 mixture of ethoxylated (20/3)-trimethylolpropanetriacrylate and trimethylolpropanetriacrylate (ETA-TTA), an ideally suitable 2PP formulation^{49,50} and pure M9 buffer media were taken as references, respectively.

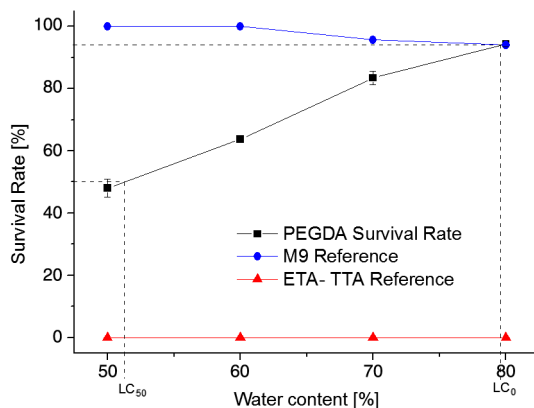


Fig. 7 Percentage of worms alive plotted against decreasing concentrations of PEGda in M9, worms kept in the uncured resin for 15 min; black line: PEGda in buffer media at different concentrations (triple measurements), blue line: buffer reference, red line: standard 2PP compound ETA-TTA.⁴⁹ Each data point represents an individual measurement performed with 300 to 400 worms. Data points in one vertical row represent experiments done at the same time with the same population. LC₅₀ and LC₀ values are highlighted.

Although the nonaqueous ETA-TTA virtually immobilized all worms, the survival rates progressively raised using decreasing amounts of PEGda in buffer media (Fig. 7). At approximately 52% water content, 50% of the worms survive when exposed for 15 min (LC₅₀). Considering the buffer reference, the survival rate increased by 33%, 35%, and 15% when raising the water content from 50% to 60%, 60% to 70%, and 70% to 80%, respectively. At 79% water content, no difference to the reference was found (LC₀).

The biocompatibility of the initiator WSPI was investigated in a control experiment. Worms in buffer media containing 2 wt.% of WSPI (the concentration used for structuring in this work) was 84% ($\pm 4\%$) at an exposure time of 15 min. The survival rate of worms in buffer reference was 93%. The animals showed no quantifiable reaction to the exposure in the investigated timeframe.

In contrast to standard 2PP formulations like ETA-TTA, PEG-based hydrogels dissolved in buffer media show higher biocompatibility. For the applied exposure time, the toxic influence of the initiator seems low.

The photopolymerizable formulation contains M9 buffer media, the monomer PEGda and the initiator WSPI. From these components, PEGda only has a quantifiable toxic influence in the investigated timeframe. Therefore, we consider the monomer as good proxy for the total biocompatibility of the formulations for the investigated timeframe. In this paper, we quantitatively define a material as being biocompatible if the survival rate of *C. elegans* in the investigated formulation exceeds 50% measured against reference animals held in pure M9 buffer media (LC₅₀) at an exposure time of 15 min.

3.5 3-D Structuring with Embedded *C. elegans*

A woodpile structure containing 50% water content was fabricated around a living *C. elegans* (Fig. 8). The polymer lines were attached to the exterior of the worm (cuticle) as the laser focus was traced through the body of the animal (see Video 1).

This data shows that PEG-based hydrogels together with WSPI combine high reactivity with sufficient biocompatibility enabling rapid biofabrication of high-resolution 3-D scaffolds with embedded living organisms.

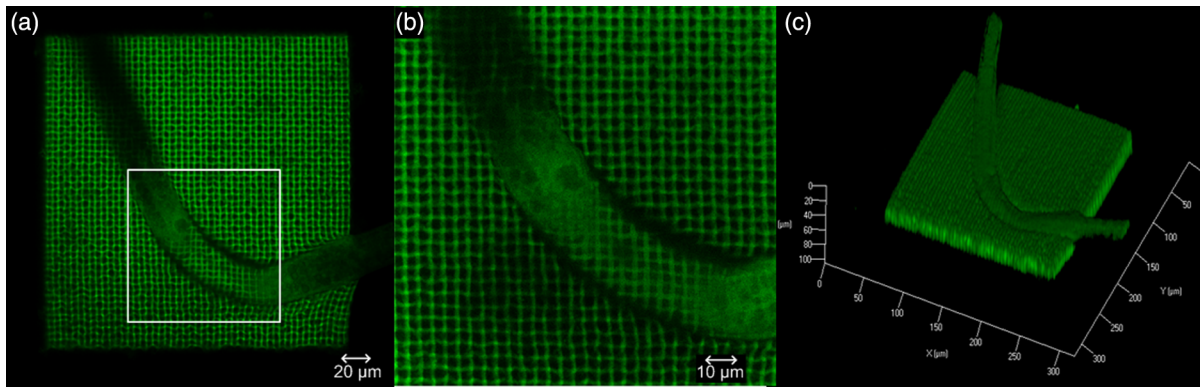


Fig. 8 *C. elegans* captured in a woodpile structure with $200\ \mu\text{m}$ side length (line distance $4\ \mu\text{m}$, layer distance $3.5\ \mu\text{m}$, 10 layers, writing speed $10\ \text{mm/s}$, laser power $220\ \text{mW}$, 50% water content). (a) LSM image 20x; (b) detail of white marked section in (a), LSM image 50x; and (c) stacked 3-D LSM image 20x (Video 1, MPG, 17.7 MB) [URI: <http://dx.doi.org/10.1117/1.JBO.17.10.105008.1>].

4 Discussion

In this paper, we present the results of studies involving the 2PP structuring of a hydrogel with embedded organisms. The material presented, PEGda in combination with a water-soluble highly efficient initiator, has advantages due to the combination of three key issues:

- (1) Processability with NIR laser light. The damage to biological tissue is negligibly low.
- (2) Water solubility allowing for high water contents in the reactive solutions. A water-based medium of choice can resemble physiologic conditions.
- (3) High reactivity resulting in a fast structuring process, reducing the exposure time to the polymerizing light while allowing high resolution.

Processability with NIR laser light: optical absorption coefficients of biologic tissues are dominated by the absorption of proteins, DNA, melanin, hemoglobin, and water. The variation of their optical activities is strongly dependent on the wavelength.⁴² In the NIR region, water is the most important tissue chromophore.⁴² It begins contributing significantly to tissue absorption at $\lambda \geq 900\ \text{nm}$.⁵⁴ Thus the heating of the tissue increases with the wavelength. Light below $800\ \text{nm}$, however, increasingly causes photochemically induced stress inside biological tissue.⁵⁴ The damage caused is significantly higher using light with wavelengths below $800\ \text{nm}$. Hence, compared to ultraviolet (UV) light, NIR light and light of $800\ \text{nm}$ in particular, seems to be more suitable for inducing polymerization in the near vicinity of biological tissues.

Potentially, laser induced photodamage can have a negative effect on biological material. In previous experiments, researchers investigating cell regulation made use of fs, NIR laser pulses to selectively ablate intracellular components in live cells without altering neighboring structures or compromising cell viability. Focusing $100\ \text{fs}$ pulsed $800\ \text{nm}$ wavelength laser light tightly ($100\times$ NA 1.4 objective) beneath cell membranes, pulse energies of $1.5\ \text{nJ}$ at process speeds of $5 \times \mu\text{m/s}$ were reported as being necessary to induce ablation.³⁴ With laser surgery, pulse energies above $2\ \text{nJ}$ of a tightly focussed ($64\times$ NA 1.4 objective) fs laser beam are necessary for severing single axons of *C. elegans*.⁵⁵ Furthermore it could be shown that two photon photodegradation of PEG hydrogels with embedded

cells can be done at pulse energies below $1.5\ \text{nJ}$, maintaining high cell viability and causing no nonspecific intracellular ablation.⁵⁶

For our experiments, we expected a laser induced photodamage on the organism being very unlikely due to the following arguments:

- (1) Given the 30% transmission efficiency of the used objective, the maximum pulse energy in the focal volume is $1.2\ \text{nJ}$ at the setup-specific laser power maximum of $300\ \text{mW}$, which is well below the reported pulse energy maximum of $1.5\ \text{nJ}$.
- (2) The larger the NA, the smaller the volume illuminated at the focal point and the lower the energy required to reach the intensity threshold for ablation.³⁴ As we use a $20\times$ NA 0.4 objective, we can expect a higher energy threshold as being necessary for nonspecific ablation.
- (3) The reported pulse energy threshold of $1.5\ \text{nJ}$ was assessed for scanning of $5\ \mu\text{m/s}$. The processing speed in this work was $10\ \text{mm/s}$, which means that the exposure time to the beam was shorter by a factor of 2000.



Fig. 9 Two-photon-polymerization in the presence of living *C. elegans*, woodpile structure $200 \times 200 \times 35\ \mu\text{m}^3$ (Video 2, MPG, 7.06 MB) [URI: <http://dx.doi.org/10.1117/1.JBO.17.10.105008.2>].

To double-check this, we exposed several specimens of *C. elegans* to the focal point of the objective at the maximum intensity for 2 to 3 s. This did not lead to any quantifiable effects compared to nonexposed controls.

Water Solubility: Our biocompatibility assay reveals that PEGda, the organic monomer, is mainly responsible for a lower chance of survival of *C. elegans* exposed to the photopolymerizable formulations. At 50% water content, the chance of survival shrinks to 50% at an exposure time of 15 min. However, the highly efficient (120 GM at 800 nm)⁴¹ 2PA initiator WSPI enables the fabrication of 3-D structures in 2PA hydrogels with water contents of 80% (Figs. 4 and 6). This limits the potentially toxic organic compounds to a minimum. Though no stable structures were obtained with 90% water, contents between 80% and 90% are likely to be functional. Furthermore, as with previous approaches,^{22,36} water-based media can be used as developer to remove residual monomers. Organic solvents can be entirely omitted.

High Reactivity: Objects were fabricated at average laser powers as low as 140 mW at 80% water content and at a speed of 10 mm/s. The performance of the presented formulations is comparable with standard organic-based formulations, where appropriate 3-D structures were built at 50 mW and 0.8 mm/s (The experiment was done using the same experimental setup and the same 20× NA 0.4 objective).⁵³ The experiments in Sec. 3.2 reveal a competitive threshold of 60 mW at 1 mm/s for 3-D fabrication in a formulation containing 50% water. The compound PEGda was already successfully cross-linked via 2PP at higher energy doses and without water content in the formulation^{22,36} using a different initiator. Thus, the reported low threshold can be attributed to the high 2PA cross-section of the initiator WSPI⁴¹ and its efficiency for cross-linking PEGda. The processability of formulations with only 20% monomer content confirms this conclusion. Due to mechanical limitations, the maximum writing speed was 10 mm/s. However, the materials presented are likely processable at higher writing speeds.

The object's deviations from the CAD model due to swelling and shrinking could limit the resolution advantage of 2PP over STL. However, our experiments show that the objects' dimension deviations can be compensated permitting to adapt the CAD model accordingly.

So far, we have defined the biocompatibility of the presented approach from two different perspectives. From the literature, a pulse energy threshold of 1.5 nJ emerges under which we should operate to prevent nonspecific ablation. Secondly, we have found out that 50% content of PEGda in the photopolymerizable formulation leads to a survival rate of 50%, whereas no quantifiable toxic effect can be observed at a content of 80% relative to the reference. Yet, we did not combine these two perspectives to actually show polymerization in the presence of a living organism. A conformable proof requires visual evidence for the formation of a polymerized construct and an evidence for the animal being alive at the same time. Thus, as we investigate the biocompatibility via movement assays,⁵² an online process observation of a 2PP structuring procedure with an embedded *C. elegans* would combine both perspectives. However, as the animal cannot be immobilized for this purpose, the experiment places several requirements to the formulation[†]:

- (1) A stiff and dense polymer network is necessary, which the animal cannot easily damage.
- (2) The viscosity must be high to limit the movement of the worm, facilitating an easier positioning and tracking without the need of the animal's immobilization.
- (3) The emerging polymer network must have a different refractive index compared with the uncured residue. Otherwise it would be hard to recognize single polymer lines online.

Though polymerization in the presence of living organisms is more biocompatible in formulations with 80% water content, the experiment would not have clearly shown a 2PP process in the presence of a living organism. A higher monomer content is necessary for visual evidence, but not for successful polymerization in principle.

The online process observation (Fig. 9, Video 2) shows that *C. elegans* survive a 2PP structuring procedure in a formulation containing 50% water. The writing speed was set to 0.3 mm/s for better observation. The power was adapted to 50 mW, a previously established appropriate power value for structuring at this writing speed. The voxel is traced through the body of the animal. As what can be seen from the online observation, this exposure to the focused beam does not trigger the animal to any specific reactions and thus does not seem to affect it (see Video 2).

Choosing *C. elegans* as a test organism provides simple and efficient means to assess the impacts of the process and the material on living organisms. The biocompatibility studies of biofabrication processes on living organisms are becoming popular because they can estimate more complex toxic effects⁴⁵⁻⁴⁷ and provide simple, efficient, and reproducible methods to predetermine the biocompatibility of their materials and methods.⁴³ Moreover, biocompatibility tests with the nematode *C. elegans* have been recently accepted by the American Society for Testing and Materials (ASTM Guide E2172-01) as standard toxicity test. *C. elegans* is an inexpensive and high-throughput biosensor. The animal's motion gave insight on its viability during the structuring process. Thus, *C. elegans* served as unique real-time biosensor for toxicity without the need of special treatment of the organism like staining or genetic modification.

The effective bio-fabrication of 3-D hydrogel scaffolds requires the combination of suitable polymerizable materials and fabrication techniques. 2PP can provide high resolution 3-D microstructures with full control over the structure details but due to the lack of suitable photoinitiators, it has not been fully implemented for structuring in biocompatible formulations with high water content. With our current work, we have shown the possibility to fabricate high resolution scaffolds from such formulations, reproducibly and directly in the presence of living organisms.

5 Conclusion

Two-photon polymerization (2PP) was performed in the presence of a living organism for the first time. The presented water soluble, 2PP initiator with a large two-photon absorption cross-section of 120 GM enabled the fabrication of complex hydrogel scaffolds at fast scanning speed of 10 mm/s and at a laser power of 140 mW. The processed formulations contained up to 80% water. *C. elegans* was used as real-time biosensor to determine the biocompatibility of the presented polymerizable

[†]Immobilization causes additional stress for *C. elegans*. This would influence the experimental findings. Furthermore, the vitality of the animal cannot be shown in an online observation.

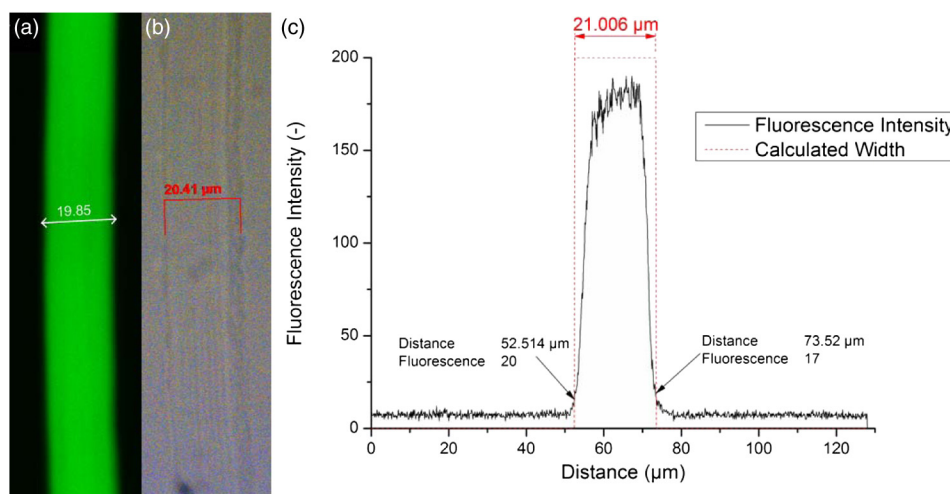


Fig. 10 Different measurement procedures (CAD rod structure according to Sec. 2.3, 240 mW, 50% water): (a) LSM 50x (b) OM 50x (c) LSM image intensity distribution.

formulations. Due to the transparency of biological tissues in the NIR spectral range, the femtosecond laser does not cause stress for the organism at the intensities reported. We anticipate that 2PP offers several advantages for *in vivo* microfabrication in tissue engineering applications, pharmaceutical assays and studies of cell behavior in 3-D environments.

Acknowledgments

The presented work was financially supported by PHOCAM (project number 260043) under the 7th framework programme for research and technological development from the EU, the China Scholarship Council (CSC) and the European Science Foundation (P2M Network). We thank Klaus Stadlmann (Vienna University of Technology) for his technical assistance on the two-photon-polymerization experimental setup as well as Antoine Baudrimont, Christian Pflügl and Alexander Woglar (Vienna Biocenter) for providing us *C. elegans*.

Appendix: Rod Width Measurements by Fluorescence Distribution over the Scanned Plane

In Fig. 10, three different approaches of rod width measurements are presented. The values obtained with laser scanning microscopy (LSM) are less than those obtained with conventional optical microscopy (OM). The superior depth of field in the LSM scan allows to precisely evaluate the width of separate layers, while the OM image represents a projection of all layers of the fabricated part. In addition, due to low contrast of the OM image it is hard to define the actual interface between the cured hydrogel structure and the surrounding buffer media. This is particularly evident for structures produced at lower laser power in formulations with higher water content. The fluorescence of the LSM images provides a quantifiable criteria—the edge of the hydrogel structure is defined as the plane where the fluorescence signal intensity exceeds the background noise by at least 10%. Following this principle, the experimental data was evaluated in an automated procedure, excluding any subjective influences.

References

1. J. Patterson, M. M. Martino, and J. A. Hubbell, "Biomimetic materials in tissue engineering," *Mater. Today* **13**(1–2), 14–22 (2010).
2. R. Langer and J. P. Vacanti, "Tissue engineering," *Science* **260**(5110), 920–926 (1993).
3. D. W. Hutmacher, "Scaffold design and fabrication technologies for engineering tissues state of the art and future perspectives," *J. Biomater. Sci.* **12**(1), 107–124 (2001).
4. T. M. Seck et al., "Designed biodegradable hydrogel structures prepared by stereolithography using poly(ethylene glycol)/poly(D,L-lactide)-based resins," *J. Control. Release* **148**(1), 34–41 (2010).
5. D. W. Hutmacher, M. Sittinger, and M. V. Risbud, "Scaffold-based tissue engineering: rationale for computer-aided design and solid free-form fabrication systems," *Trends Biotech.* **22**(7), 354–362 (2004).
6. W.-Y. Yeong "Rapid prototyping in tissue engineering: challenges and potential," *Trends Biotech.* **22**(12), 643–652 (2004).
7. F. P. W. Melchels, J. Feijen, and D. W. Grijpma, "A review on stereolithography and its applications in biomedical engineering," *Biomaterials* **31**(24), 6121–6130 (2010).
8. P. J. Bártolo, *Stereolithography: Materials, Processes and Applications*, Springer, New York (2011).
9. A. Khademhosseini and R. Langer, "Microengineered hydrogels for tissue engineering," *Biomaterials* **28**(34), 5087–5092 (2007).
10. I. Tomatsu, K. Peng, and A. Kros, "Photoreponsive hydrogels for biomedical applications," *Adv. Drug Deliv. Rev.* **63**(14–15), 1257–1266 (2011).
11. M. W. Tibbitt and K. S. Anseth, "Hydrogels as extracellular matrix mimics for 3-D cell culture," *Biotechnol. Bioeng.* **103**(4), 655–663 (2009).
12. J.-T. Schantz et al., "Osteogenic differentiation of mesenchymal progenitor cells in computer designed fibrin-polymer-ceramic scaffolds manufactured by fused deposition modeling," *J. Mater. Sci.* **16**(9), 807–819 (2005).
13. J. M. Williams et al., "Bone tissue engineering using polycaprolactone scaffolds fabricated via selective laser sintering," *Biomaterials* **26**(23), 4817–4827 (2005).
14. B. Dhariwala, E. Hunt, and T. Boland, "Rapid prototyping of tissue-engineering constructs, using photopolymerizable hydrogels and stereolithography," *Tissue Eng.* **10**, 1316–1322 (2004).
15. K. Arcaute, B. K. Mann, and R. B. Wicker, "Stereolithography of three-dimensional bioactive poly(ethylene glycol) constructs with encapsulated cells," *Ann. Biomed. Eng.* **34**(9), 1429–1441 (2006).
16. L. Moroni et al., "3-D fiber-deposited electrospun integrated scaffolds enhance cartilage tissue formation," *Adv. Funct. Mater.* **18**, 53–60 (2008).
17. V. L. Tsang et al., "Fabrication of 3-D hepatic tissues by additive photopatterning of cellular hydrogels," *FASEB J.* **21**(3), 790–801 (2007).

18. N. E. Fedorovich et al., "The effect of photopolymerization on stem cells embedded in hydrogels," *Biomaterials* **30**(3), 344–353 (2009).
19. A. M. Kloxin et al., "Photodegradable hydrogels for dynamic tuning of physical and chemical properties," *Science* **324**(5923), 59–63 (2009).
20. R. P. Sinha and D. P. Häder, "UV-induced DNA damage and repair: a review," *Photochem. Photobiol. Sci.* **1**(4), 225–236 (2002).
21. A. Ovsianikov et al., "Laser fabrication of three-dimensional CAD scaffolds from photosensitive gelatin for applications in tissue engineering," *Biomacromolecules* **12**(4), 851–858 (2011).
22. A. Ovsianikov et al., "Three-dimensional laser micro- and nano-structuring of acrylated poly(ethylene glycol) materials and evaluation of their cytotoxicity for tissue engineering applications," *Acta Biomater.* **7**(3), 967–974 (2011).
23. A. Ovsianikov et al., "Two-photon polymerization technique for microfabrication of CAD-designed 3-D scaffolds from commercially available photosensitive materials," *J. Tissue Eng. Regen. Med.* **1**, 443–449 (2007).
24. A. Ovsianikov et al., "Engineering 3D cell-culture matrices: multi-photon processing technologies for biological & tissue engineering applications," *Expert. Rev. Med. Dev.*, 1–21 (2012).
25. H. Sun and S. Kawata, "Two-photon photopolymerization and 3D lithographic microfabrication," in *NMR, 3D Analysis, Photopolymerization, Advances in Polymer Science*, pp. 169–274, Springer, Berlin/Heidelberg (2004).
26. C. W. Hull et al., "Apparatus and related method for forming a substantially flat stereolithographic working surface," U. S. Patent 5447822 (1995).
27. C. W. Hull, "Apparatus for production of three-dimensional objects by stereolithography," U. S. Patent 4575330 (1986).
28. A. K. O'Brien, N. B. Cramer, and C. N. Bowman, "Oxygen inhibition in thiol-acrylate photopolymerizations," *J. Polymer Sci. A* **44**, 2007–2014 (2006).
29. D. A. Parthenopoulos and P. M. Rentzepis, "Two-photon volume information storage in doped polymer systems," *J. Appl. Phys.* **68**(11), 5814–5818 (1990).
30. W. Haske et al., "65 nm feature sizes using visible wavelength 3-D multiphoton lithography," *Opt. Express* **15**(6), 3426–3436 (2007).
31. S.-H. Park, D.-Y. Yang, and K.-S. Lee, "Two-photon stereolithography for realizing ultraprecise three-dimensional nano/microdevices," *Laser Photon. Rev.* **3**(1–2), 1–11 (2009).
32. P. Lenz, "In vivo excitation of photosensitizers by infrared light," *Photochem. Photobiol.* **62**(2), 333–338 (1995).
33. W. Denk, J. Strickler, and W. W. Webb, "Two-photon laser microscopy," U. S. Patent 5034613 (1991).
34. N. Shen et al., "Ablation of cytoskeletal filaments and mitochondria in live cells using a femtosecond laser nanoscissor," *Mech. Chem. Biosyst.* **2**(1), 17–25 (2005).
35. W. Watanabe et al., "Femtosecond laser disruption of subcellular organelles in a living cell," *Opt. Express* **12**(18), 4203–4213 (2004).
36. A. Berg et al., "Synthesis of photopolymerizable hydrophilic macromers and evaluation of their applicability as reactive resin components for the fabrication of three-dimensionally structured hydrogel matrices by 2-photon-polymerization," *Adv. Eng. Mater.* **13**(9), B274–B284 (2011).
37. T. Kawano et al., "PNIPAM gel-coated gold nanorods for targeted delivery responding to a near-infrared laser," *Bioconjugate Chem.* **20**(2), 209–212 (2009).
38. P. J. Campagnola et al., "3-dimensional submicron polymerization of acrylamide by multiphoton excitation of xanthene dyes," *Macromolecules* **33**(5), 1511–1513 (2000).
39. S. Basu et al., "Multiphoton-excited microfabrication in live cells via Rose Bengal-cross-linking of cytoplasmic proteins," *Opt. Lett.* **30**(2), 159–161 (2005).
40. X. Wan et al., "Water-soluble benzylidene cyclopentanone dye for two-photon photopolymerization," *J. Photochem. Photobiol. A* **202**(1), 74–79 (2009).
41. H. Y. Woo et al., "Solvent effects on the two-photon absorption of distyrylbenzene chromophores," *J. Am. Chem. Soc.* **127**(42), 14721–14729 (2005).
42. G. Leitz et al., "Stress response in *Caenorhabditis elegans* caused by optical tweezers: wavelength, power, and time dependence," *Biophys. J.* **82**(4), 2224–2231 (2002).
43. J. D. W. Clarke and S. N. Jayasinghe, "Bio-electrosprayed multicellular zebrafish embryos are viable and develop normally," *Biomed. Mater.* **3**(1), 011001 (2008).
44. P. L. Williams and D. B. Dusenbery, "Using the nematode *Caenorhabditis elegans* to predict mammalian acute lethality to metallic salts," *Toxicol. Ind. Health* **4**(4), 469–478 (1998).
45. S. Donkin and D. Dusenbery, "A soil toxicity test using the nematode *Caenorhabditis elegans* and an effective method of recovery," *Arch. Env. Contamin. Toxicol.* **25**(2), 145–151 (1993).
46. S. G. Donkin and D. B. Dusenbery, "Using the *Caenorhabditis elegans* soil toxicity test to identify factors affecting toxicity of four metal ions in intact soil," *Water Air Soil Poll.* **78**(3–4), 359–373 (1994).
47. C. I. Bargmann, "Chemosensation in *C. elegans*," 25 Oct 2006," in *WormBook: The Online Review of C. elegans Biology*, WormBook, Pasadena, CA (2005).
48. B. H. Cumpston et al., "Two-photon polymerization initiators for three-dimensional optical data storage and microfabrication," *Nature* **398**, 51–54 (1999).
49. N. Pucher et al., "Structure-activity relationship in D- π -A- π -D-based photoinitiators for the two-photon-induced photopolymerization process," *Macromolecules* **42**(17), 6519–6528 (2009).
50. Z. Li et al., "Synthesis and structure-activity relationship of several aromatic ketone-based two-photon initiators," *J. Polymer Sci. A* **49**(17), 3688–3699 (2011).
51. S. Brenner, "The genetics of *Caenorhabditis elegans*," *Genetics* **77**(1), 71–94 (1974).
52. L. J. Bischof, D. L. Huffman, and R. V. Aroian, "Assays for toxicity studies in *C. elegans* with Bt crystal proteins," in *C. Elegans*, pp. 139–154, Humana Press, New Jersey (2006).
53. K. Cicha et al., "Evaluation of 3-D structures fabricated with two-photon-photopolymerization by using FTIR-spectroscopy," *J. Appl. Phys.* **110**(6), 064911 (2011).
54. A. Vogel and V. Venugopalan, "Mechanisms of pulsed laser ablation of biological tissues," *Chem. Rev.* **103**(2), 577–644 (2003).
55. M. W. Tibbitt et al., "Controlled two-photon photodegradation of PEG hydrogels to study and manipulate subcellular interactions on soft materials," *Soft Mater.* **6**, 5100–5108 (2010).
56. M. F. Yanik et al., "Neurosurgery: functional regeneration after laser axotomy," *Nature* **432**(7019), 822–822 (2004).
57. W. A. N. Dorland, *Dorland's Illustrated Medical Dictionary*, Saunders, Philadelphia, PA/London (2011).